

FRactal sub-grid scale model for large eddy simulation of atmospheric turbulence: A *PRIORI* study

Emmanuel O. Akinlabi
Institute of Geophysics,
Faculty of Physics,
University of Warsaw, Warsaw, Poland
Email: emmanuel.akinlabi@fuw.edu.pl

Marta Waclawczyk
Institute of Geophysics,
Faculty of Physics,
University of Warsaw, Warsaw, Poland
Email: marta.waclawczyk@fuw.edu.pl

Szymon P. Malinowski
Institute of Geophysics,
Faculty of Physics,
University of Warsaw, Warsaw, Poland
Email: malina@igf.fuw.edu.pl

Juan Pedro Mellado
Max-Planck Institute for Meteorology,
Hamburg, Germany
Email: juan-pedro.mellado@mpimet.mpg.de

ABSTRACT

We present a fractal sub-grid scale model for large eddy simulation (LES) of atmospheric convective boundary layer flow. This model is based on the fractality assumption of turbulent velocity field. It reconstructs sub-grid velocity field from the knowledge of its filtered values on LES coarse grid, by means of fractal interpolation, proposed by Scotti and Meneveau (1999). The characteristics of the reconstructed signal depend on the stretching parameters d , which is related to the fractal dimension of the signal. Previous studies assume a constant stretching parameter in space and time. To improve the fractal interpolation approach, we account for the stretching parameter variability. We calculate the local stretching parameters from direct numerical simulation (DNS) data of convective boundary layer using an algorithm proposed by Mazel and Hayes (1992) and compute its probability density function (PDF). We found that the PDFs of d have a universal form when the velocity field is filtered to wave-numbers within the inertial range. It is assumed that the stretching parameter d is a random variable with the inertial range PDF of d . We perform 1D *a priori* test and compare energy spectra and statistics of velocity increments with DNS data.

1 INTRODUCTION

Complex spatial and temporal structures are the major features seen in atmospheric flows. These structures are seen over a wide range of scales from large synoptic scales $\mathcal{O}(1000\text{km})$ to the smallest dissipative scales $\mathcal{O}(1\text{cm} - 1\text{mm})$ with their ratio $L/\eta \approx \mathcal{O}(10^9)$. All scales play an important role in weather prediction especially the small scales, which influence particle statistics such as preferential concentration, average settling velocity and relative velocities. Direct numerical simulation (DNS) is an ideal approach to resolve all these scales but it imposes an unrealistic computational cost. Alternatively, large-eddy simulation (LES) allows for significantly improved accuracy in simulating atmospheric (turbulent) flows, by calculating the large scale features of the flow while the interactions be-

tween large (resolved) scales and small (unresolved) scales are accounted for by a subgrid-scale model.

Structural sub-grid models such as fractal interpolation technique (FIT) was introduced to construct synthetic, fractal subgrid-scale fields applied to large eddy simulation (Scotti & Meneveau, 1999). This model was aimed at mimicking (some of) the subgrid scales. It also allows for the approximate reconstruction of two-point particle statistics at the subgrid scale, such as relative small scale velocity and particle segregation patterns (Minier & Pozorski, 2017). This sub-grid model has been shown to be computationally efficient and easy to use (Akinlabi *et al.*, 2019). The model's underlying assumption is the existence of fractal-scale similarity of velocity fields. An attribute of the constructed sub-grid velocity depends on the stretching parameter d , which is related to the fractal dimension of the signal. In Scotti & Meneveau (1999), it was assumed that d is constant in space and time. These parameters were set to $d = \pm 2^{-1/3}$ derived from $-5/3$ inertial range scaling of turbulence. Basu *et al.* (2004) Basu *et al.* (2004) proposed an extension of this work by developing a multi-affine fractal interpolation scheme with stretching parameters $d = -0.887$ and $d = -0.676$ and showed that it preserves the higher-order structure functions and the non-Gaussian probability density function of the velocity increments. They performed an extensive *a priori* analyses of atmospheric boundary layer measurements and argued that the multi-affine closure model should give satisfactory performance in large eddy simulations.

Characteristic features of atmospheric turbulence such as the convective boundary layer are the inhomogeneity due to buoyancy and the presence of internal and external intermittency. External intermittency refers to the co-existence of both laminar and turbulent regions in the flow. Internal intermittency means that at small scales, large velocity gradients are present and the PDF of velocity differences at high Reynolds number is stretched-exponential (Ishihara *et al.*, 2009). These attributes are the main set back of FIT since the local stretching parameters have been shown to change randomly in space and time (Akinlabi *et al.*, 2018;

Marchioli, 2017). The aim of this work is to develop an improvement to FIT, which can be used as a closure model for Lagrangian tracking of particles in atmospheric turbulence. First, we account for the variability of the stretching parameter by computing its local value with an algorithm proposed by Mazel & Hayes (1992). Then, the PDF of local stretching parameter is used to construct subgrid velocity, starting with the filtered DNS of convective boundary layer flow (Mellado *et al.*, 2016). The PDF of d is used to perform 1D reconstruction of subgrid eddies. We compare the performance of the new approach with Scotti & Meneveau (1999) approach and the multiaffine fractal interpolation scheme (Basu *et al.*, 2004), which use constant stretching parameters. We calculate the energy spectra of the reconstructed velocity field and the statistics of velocity increments. The focus on the statistics of velocity increments is motivated by their ability to quantify internal intermittency of small scale turbulence (Ishihara *et al.*, 2009; Kamps *et al.*, 2009; Lui *et al.*, 2010). We found the new approach with random d the most favourable in terms of the investigated statistics. It reproduces the Kolmogorov's $-5/3$ scaling of turbulent kinetic energy spectra in the inertial range with the smallest error and without spurious modulations. Moreover, PDFs of increments of the reconstructed velocity have non-Gaussian, stretched-exponential tails and agrees well with DNS.

2 FRACTAL INTERPOLATION TECHNIQUES

2.1 Basics

The fractal interpolation technique is an iterative affine mapping procedure to construct the synthetic (unknown) small-scale eddies of the velocity field $\mathbf{u}(\mathbf{x}, t)$ from the knowledge of a filtered or coarse-grained field $\tilde{\mathbf{u}}(\mathbf{x}, t)$ (Scotti & Meneveau, 1999). For instance, if $\tilde{\mathbf{u}}(\mathbf{x}, t)$ have resolution Δ' while $\tilde{\mathbf{u}}(\mathbf{x}, t)$ have Δ such that $\Delta' > \Delta$, the mapping operator $W[\cdot]$ applied to $\tilde{\mathbf{u}}(\mathbf{x}, t)$ gives $\tilde{\mathbf{u}}(\mathbf{x}, t) = W[\tilde{\mathbf{u}}(\mathbf{x}, t)]$. The mapping is performed many times to generate synthetic small scale velocity fields i.e. a fractal synthetic field

$$\begin{aligned} \mathbf{u}_f(\mathbf{x}, t) &= \lim_{n \rightarrow \infty} W^{(n)}[\tilde{\mathbf{u}}(\mathbf{x}, t)] \\ &\equiv \lim_{n \rightarrow \infty} W[W[W \dots W[\tilde{\mathbf{u}}(\mathbf{x}, t)] \dots]] \end{aligned}$$

For example, if we consider three interpolating points $\{(x_i, \tilde{u}_i), i = 0, 1, 2\}$, the fractal interpolation reconstructs a signal w_j , $j = 1, 2$ at two additional points placed between points 0 and 1 and points 1 and 2, see figure 1. Here, w_j has the following transformation structure:

$$w_j \begin{pmatrix} x \\ u \end{pmatrix} = \begin{bmatrix} a_j & 0 \\ c_j & d_j \end{bmatrix} \begin{pmatrix} x \\ u \end{pmatrix} + \begin{pmatrix} e_j \\ f_j \end{pmatrix}, \quad j = 1, 2 \quad (1)$$

with constraints

$$w_j \begin{pmatrix} x_0 \\ \tilde{u}_0 \end{pmatrix} = \begin{pmatrix} x_{j-1} \\ \tilde{u}_{j-1} \end{pmatrix} \quad \text{and} \quad w_j \begin{pmatrix} x_2 \\ \tilde{u}_2 \end{pmatrix} = \begin{pmatrix} x_j \\ \tilde{u}_j \end{pmatrix}, \quad j = 1, 2 \quad (2)$$

The parameters a_j, c_j, e_j and f_j can be written in terms of d_j (called the stretching parameter) and the interpolation points $\{(x_i, \tilde{u}_i), i = 0, 1, 2\}$. Values of d_j fix the vertical stretching of the left and right segments at each iteration and

determine characteristics of the reconstructed signal. Their values are independent of the interpolation points.

The iterative procedure in the limit $n \rightarrow \infty$ creates a continuous function $\mathbf{u}_f(\mathbf{x})$ provided that the stretching parameter d_j obeys $0 \leq |d_j| < 1$. Also, if $|d_1| + |d_2| > 1$ and (x_i, \tilde{u}_i) , are not collinear, then the fractal dimension D of the reconstructed signal is the unique real solution of $|d_1|a_1^{D-1} + |d_2|a_2^{D-1} = 1$ (for proof, see Barnley (1986)). Another important constraint is that a fractal signals only dissipate energy in the limit of small viscosity if $|d| > 0.5$ (Scotti *et al.*, 1995). Thus, once the stretching parameter is chosen, the remaining parameters a_j, c_j, e_j and f_j are given as

$$a_j = \frac{x_j - x_{j-1}}{x_2 - x_0} \quad (3)$$

$$e_j = \frac{x_2 x_j - x_0 x_j}{x_2 - x_0} \quad (4)$$

$$c_j = \frac{\tilde{u}_j - \tilde{u}_{j-1}}{x_2 - x_0} - d_j \frac{\tilde{u}_2 - \tilde{u}_0}{x_2 - x_0} \quad (5)$$

$$f_j = \frac{x_2 \tilde{u}_{j-1} - x_0 \tilde{u}_j}{x_2 - x_0} - d_j \frac{x_2 \tilde{u}_0 - x_0 \tilde{u}_2}{x_2 - x_0} \quad (6)$$

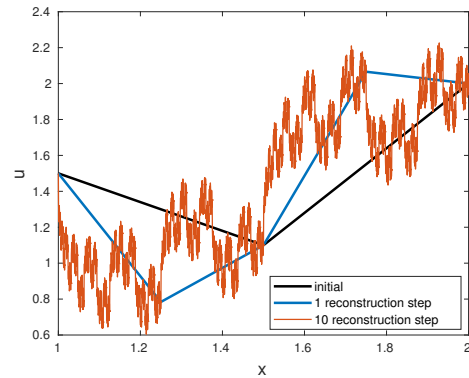


Figure 1. Different stages during the construction of a fractal function with stretching parameter $d = \pm 2^{-1/3}$ after 0, 1 and 10 reconstruction steps.

Given that

$$1 < \sum_{j=1}^N |d_j| < 2, \quad (7)$$

where $N + 1 = N_A$ and N_A is the number of anchor points (here, $N = 2$), the stretching parameter d_j relates to the fractal dimension D of a velocity field as:

$$D = 1 + \log_N \sum_{j=1}^N |d_j| \quad (8)$$

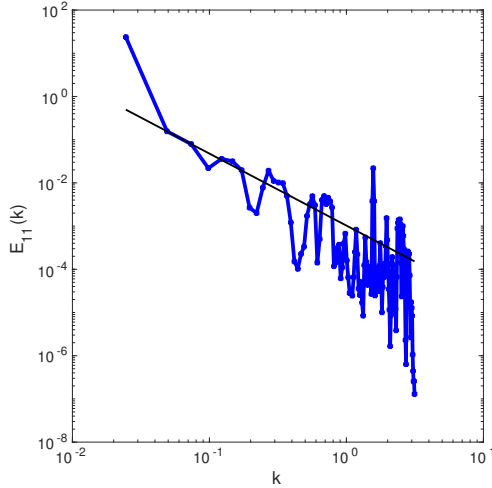


Figure 2. Energy spectrum of the reconstructed signal after 10 iterations showing $-5/3$ slope.

(for proof, see Barnley (1993)). It is important to point out that the relation between inertial-range self-similarity of turbulent velocity field and the fractal dimension is not trivial. This relation is given by Orey (Orey, 1970) for Gaussian random fields with a power-law spectrum, $E(k) \sim k^{-\alpha}$ with $1 < \alpha < 3$. The fractal dimension is given as $D = (5 - \alpha)/2$. For Kolmogorov spectrum, $\alpha = 5/3$, which results in $D = 1.67$. Although turbulent velocity fluctuations are not Gaussian, the high-Reynolds experimental results of Praskovskiy *et al.* (1993) and Scotti *et al.* (1995) have a fractal dimension $D \simeq 1.7 \pm 0.05$, which agrees closely with Orey's theorem.

If a fractal dimension of $5/3$ relating to $-5/3$ Kolmogorov scaling in the inertial-range of velocity fields is assumed, then $d_j = \pm 2^{-1/3}$ (if d_j is assumed to be the same for all grid spacings) (Scotti & Meneveau, 1999). Figure 1 shows the 1-D construction of w_j . We start from a field with three grid points and we successively apply the map w_j with stretching parameter $d_j = \pm 2^{-1/3}$. Shown are the initial field, first and the tenth application of the map w_j . The energy spectrum after ten reconstruction steps is shown in figure 2.

2.2 Stretching parameter estimation

To compute the local stretching parameter of any arbitrary dataset, Mazel & Hayes (1992) algorithm can be applied. The algorithm is based on the property that the fractal field is self-similar. For example, if we consider a dataset with 5 interpolation points $\{(x_i, u_i), i = 0, 1, 2, 3, 4\}$, let μ be the vertical distance between the middle interpolation point (x_2, u_2) and a straight line between the end points (x_0, u_0) and (x_4, u_4) , see figure 3. The value of μ is positive if the interpolation points are above the straight line and negative otherwise. Let τ_1 be the vertical distance between (x_1, u_1) and a straight line between (x_0, u_0) and (x_2, u_2) while τ_2 be the vertical distance between (x_3, u_3) and a straight line between (x_2, u_2) and (x_4, u_4) . Both τ_1 and τ_2 are positive if their respective interpolation points are above their respective straight lines and negative otherwise. Then the stretching parameters d_1 and d_2 are τ_1/μ and τ_2/μ , respectively. An illustration of this calculation is presented in figure 3.

In Akinlabi *et al.* (2018, 2019), it was shown that for

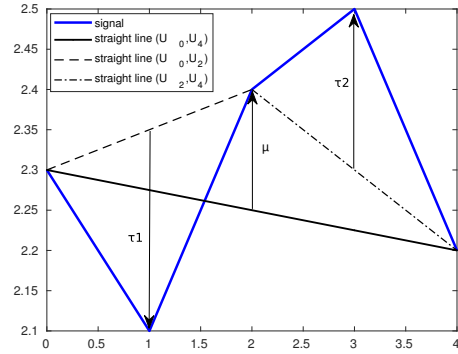


Figure 3. Illustration of the stretching parameter calculation.

any arbitrary signal, the original and FIT signal are identical if the Mazel & Hayes (1992) algorithm is used to retrieve d . Also, the stretching parameter varies significantly in space and has values outside the interval $(-1, 1)$ because the signal used is highly intermittent. In the formulation of FIT (as shown in section 2.1), d can only take values within the interval $(-1, 1)$ and hence, we place a constraint $|d| \leq 1$. This implies that only some of the magnitude of sub-grid scales will mimic the original signal.

3 TEST CASE - CONVECTIVE BOUNDARY LAYER

3.1 Description

The Mazel & Hayes (1992) algorithm was applied on DNS of a dry, shear-free convective boundary layer (CBL) that grows into a linearly stratified atmosphere (cf. figure 4). Details of the simulation can be found in Mellado *et al.* (2016). The flow is driven by a constant and homogeneous surface buoyancy flux B_0 , and the buoyancy stratification of the free atmosphere is N^2 , where N is the buoyancy frequency. This configuration is representative of mid-day atmospheric conditions over land. At a time-step, when the initial conditions have been sufficiently forgotten, statistical properties of the flow can be expressed in terms of the Prandtl number ν/κ , the Reynolds number $B_0/(N^2\nu)$, the normalized vertical distance to the surface z/h and the ratio h/L_0 where $B_0 = 0.005$ and $N^2 = 3.0$ in simulation units. The ratio h/L_0 increases as the CBL grows into the linearly stratified atmosphere. The variable $h(t)$ is defined as $h \simeq (2B_0N^{-2}t)^{1/2}$ and provides a measure of the CBL depth. The parameter $L_0 = (B_0/N^3)^{1/2} = 0.031$ is the reference Ozmidov scale. It provides a measure of the thickness of transition layer at the top of the entrainment zone between the turbulent boundary layer and the free atmosphere. The CBL depth h is about $20L_0$ and its velocity scale $U_0 = L_0N = 0.0537$. The only parameter whose atmospheric value cannot be matched with the simulation is the Reynolds number; for the data considered in this analysis, $Re_0 = 117$. The number of grid points used in the simulation is $5120 \times 5120 \times 1024$, in the streamwise, spanwise and vertical directions, respectively.

3.2 Probability distribution function of the stretching parameter

For the DNS data described in Section 3.1, we use horizontal profiles of the u , v and w components of velocity at

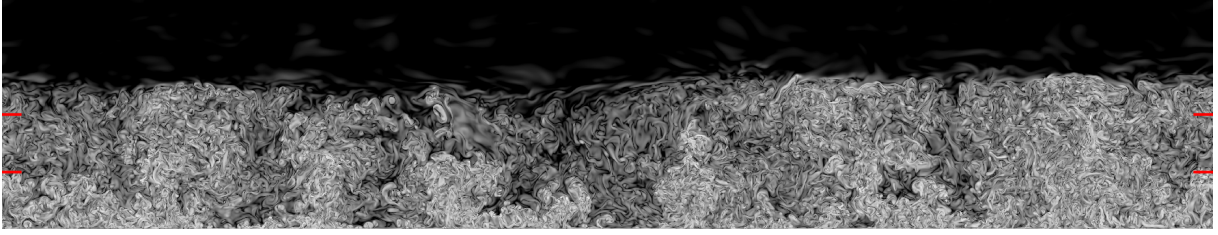


Figure 4. Vertical cross section of the logarithm of the enstrophy in the convective boundary layer. The horizontal bars at the side of the figures indicate a height equal to the CBL depth h and equal to half of it.

a height $z = 0.43h$. We choose this height because it is sufficiently far from the surface and from the height $z = 1.14h$ (which corresponds to the height of minimum buoyancy flux). First, we investigate the variability of d as 1-D intersections of DNS velocity field are filtered successively to wavenumber in the inertial range. Starting with the fully resolved DNS field with the grid spacing equal to η (where η is the smallest dissipative eddy size), we reduce the resolution to 2η by using a low-pass filter and calculate the local values of d for the filtered velocity field. Then, the velocity signal is filtered to a grid resolution of 4η etc., the cut-off wavenumber is decreased until the resolution matches the inertial-range (at about 16η to 128η). The low-pass filter used is the finite impulse response (FIR) filter of order 30 designed using the Hamming window method (Weinstein *et al.*, 1979). This is done with decimate function in MATLAB software. We use the decimation low-pass filter because it is constructed to downsample the signal (i.e. reduce the number of grid points) and guard against aliasing. The downsampling feature of the filter was important to have a reconstructed signal with the same number of grid points as the original (DNS) signal. We calculate the local estimate of d with the Mazel & Hayes (1992) algorithm explained in section 2.2. After each filtering, the local values of d were extracted, values outside the interval $(-1, 1)$ were neglected and absolute value of d was used to calculate its PDF. Since the flow is statistically homogeneous over horizontal planes, similar results were obtained for 1D intersections of velocity field calculated either in x - or y - directions. The PDF of $|d|$ and average fractal dimension of DNS velocity signals at different grid resolutions are presented in Figure 5. In figure 5a, the PDFs change significantly for the first four successive filtering steps but seem to be self-similar when filtered successively to inertial-range wavenumbers (at steps 4 to 7). PDF of d was also reported by Akinlabi *et al.* (2019) to be self-similar and independent of Reynolds' number for DNS, LES of the stratocumulus boundary layer and airborne data of Physics of Stratocumulus top (POST). This implies that the PDF of d can be used for FIT rather than the constant values of d . All three velocity components give similar profiles of the PDF of the stretching parameter. The average fractal dimension, calculated according to Eq. (8), decreases to $5/3$ inertial range scaling, as seen in figure 5b. Filtering the DNS velocity signal to grid resolution 16η or 32η corresponds to the inertial-range and we observe that their fractal dimensions $D \simeq 1.7 \pm 0.1$ agrees with Orey's theorem, slightly larger than Scotti *et al.* (1995) estimate. We also observe that probabilities of having positive or negative stretching parameter are equal.

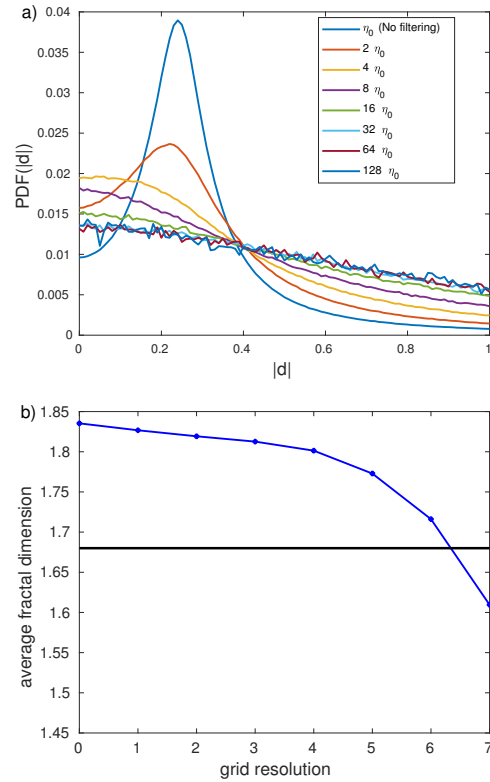


Figure 5. (a) PDFs of the absolute value of stretching parameter for horizontal profile of DNS velocity at different resolutions. (b) The average fractal dimension for horizontal profile of DNS velocity at different resolutions. The black line shows the value corresponding to the $-5/3$ inertial-range scaling.

4 RESULTS

To show the performance of the new approach, we apply FIT to a filtered 1D horizontal intersections of DNS of convective boundary layer flow (explained in section 3.1) at height $z = 0.43h$. First, the DNS velocity signal was filtered to a spatial resolution of 16η (which is within the inertial range) using the decimation function described in Section 3.2. We then reconstruct sub-filter scales back to the resolution η using FIT. For this, we select the stretching parameter from its PDF calculated from the filtered DNS data (filtered to inertial range scale where there is self-similarity of the PDF), see Fig. 5a, using the inverse transform sampling method (Devroye, 1986). The procedure is as follows

1. Calculate cumulative distribution function $F(|d|)$ from

the PDF $f(|d|)$, as

$$F(|d|) = \int_0^{|d|} f(s) ds.$$

2. Calculate the inverse function $F^{-1}(y)$.
3. If y is a random number from uniform distribution $[0,1]$ then $d = F^{-1}(y)$ is a random number from the investigated PDF.

Apart from the mathematical constraint $|d| \leq 1$, which assures the continuity of the reconstructed signal at $n \rightarrow \infty$ reconstruction steps (Barnley, 1986), the second constraint, discussed in Section 2.1 was related to the dissipative properties of the signal (Scotti *et al.*, 1995) and reads $|d| > 0.5$. Hence, in practice, in the reconstruction process, we only retained the values $|d|$ that were larger than 0.5. If $|d| \leq 0.5$ is selected, the procedure was repeated and another random value was chosen, till the condition $0.5 < |d| \leq 1$ was satisfied. Next, the sign of d was selected randomly, such that the positive and negative d have equal probabilities. Under such assumptions the ensemble average $\langle |d| \rangle$ is comparable to values reported in Ref. (Salveti *et al.*, 2006) and the scaling of the reconstructed energy spectra is close to the theoretical $k^{-5/3}$.

The inertial-range scale invariance is the property that directly relates to the idea of fractality of velocity field. As observed in Fig. 5a, profiles of PDF $f(|d|)$ display self-similarity only for cut-off wavenumbers from the inertial range. For this reason, the fractal reconstruction of the dissipative part of the spectrum is not justified, as no self-similarity is observed there. Instead, in the FIT reconstruction process, the inertial range was extended down to η and properties of such an artificial velocity field were investigated.

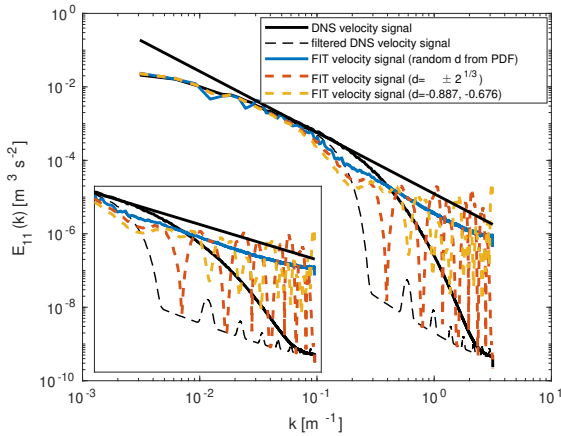


Figure 6. Longitudinal energy spectra of u velocity component for DNS and FIT with constant stretching parameter $d = \pm 2^{-1/3}$, with constant stretching parameters $d = -0.887$ and $d = -0.676$ and with random stretching parameters from calculated PDF

Figure 6 shows the longitudinal energy spectra $E_{11}(k)$ (for u velocity component along x direction) of DNS, filtered and FIT-reconstructed velocity field for the three investigated versions of the model: with $d = \pm 2^{1/3}$ as originally proposed by Scotti & Meneveau (1999), with $d_1 =$

-0.887 , $d_2 = -0.676$ as proposed by Basu *et al.* (2004), and with the new proposal with random d . As it is observed, the energy spectra of constant values of d exhibit periodic modulations (see also figures 7 and 8 of Scotti & Meneveau (1999)). Basu *et al.* (2004) avoid this modulation by applying the discrete Haar wavelet transform. FIT energy spectrum with constant values of $d = \pm 2^{1/3}$ is much lower in some wave-numbers than the $-5/3$ inertial-range scaling (especially at wavenumbers close to the cut-off scale), although the upper envelope qualitatively follows the $-5/3$ inertial-range scaling. The FIT energy spectrum reconstructed with constant values of $d = -0.887$, -0.676 has similar properties as the Scotti & Meneveau approach, except that the range between the upper and lower envelope of the spectrum is somewhat smaller. The FIT energy spectrum reconstructed with random values of d follows the inertial-range scaling closer and shows no periodic modulation.

Next, we investigated statistics of velocity increments at two different points $\mathbf{u}(\mathbf{x} + \mathbf{r}, t) - \mathbf{u}(\mathbf{x}, t)$. The sample space of velocity increment will be denoted by $\delta \mathbf{u}$ and the distance between points by $r = |\mathbf{r}|$. The tails of the PDFs of velocity increments in the isotropic turbulence $f(\delta u, r, t)$, can be approximated by the stretched exponentials. The non-Gaussianity of the PDFs for small r indicates the presence of the internal intermittency, that is, the probability of extreme events (large velocity differences) at these scales is much higher than predicted by a Gaussian distribution.

Figure 7 presents the PDFs of velocity increment (δu) for DNS, filtered DNS and FIT velocity signals with constant and random values of d for $r = 8\eta$ and $r = 2\eta$.

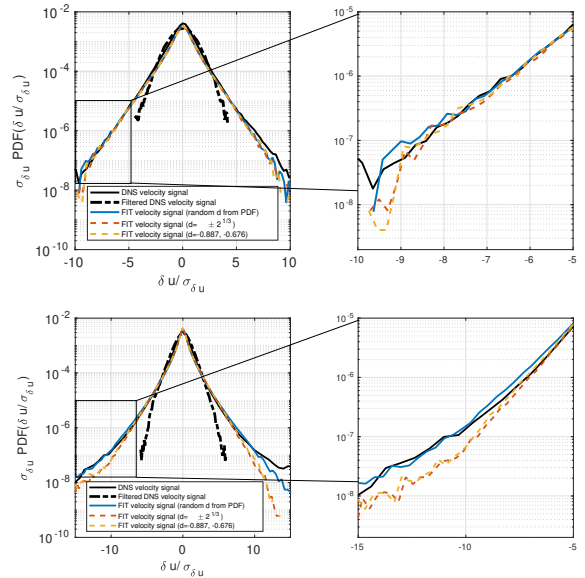


Figure 7. PDFs of velocity increments of DNS, filtered DNS and FIT fields at $r = 8\eta$ (up) and $r = 2\eta$ (down).

The PDFs of velocity increments are far from Gaussian and slightly skewed. The FIT model with random d provides the best FIT with the DNS at smaller r . We note here that at $r = 8\eta$, the difference between the three approaches is not obvious but at smaller values of r such as $r = 2\eta$, the random d correctly reproduce DNS. Although in the reconstruction process, the dissipative range (i.e. at

$r = 2\eta$) is not reproduced in any FIT model. We report here this result which seems interesting.

CONCLUSION

In this work, a fractal subgrid-scale model for large eddy simulation of atmospheric flows was presented. With fractal interpolation technique, we construct synthetic sub-grid velocity field from the knowledge of its filtered values on LES grid proposed by Scotti & Meneveau (1999). For the construction process, values of the stretching parameter d should be specified. The stretching parameter determines the characteristics of the reconstructed signal which can be derived from the fractal dimension (Scotti & Meneveau, 1999). In previous literature, the stretching parameter is chosen to be constant in time and space. To account for its spatial variability, we estimate the spatial pdf of the absolute stretching parameter $|d|$ from DNS data of convective boundary layer. First, 1D intersections of DNS velocity field was filtered with a low-pass filter to certain cut-off wavenumbers. Next, an algorithm proposed by Mazel & Hayes (1992) is used to compute the local values of d . It was found that if the cut-off wavenumbers were in the inertial range, the PDFs of the stretching parameter display self-similarity.

Next, 1D intersections of filtered DNS velocity field were reconstructed such that d is a random variable with the prescribed, previously determined PDF. Performance of the new approach was compared with FITs with constant values of d . It was shown the energy spectra follow the $-5/3$ scaling more closely and have no spurious modulations if d is random. Moreover, the non-Gaussian, stretched-exponential tails of PDFs of velocity increments are reproduced correctly by the improved model. We investigated these statistics as they quantify internal intermittency of small scale turbulence (Ishihara *et al.*, 2009; Lui *et al.*, 2010).

ACKNOWLEDGEMENT

This work received funding from the European Union Horizon 2020 Research and Innovation Programme under the Marie Skłodowska-Curie Actions, Grant Agreement No. 675675.

MW and SPM acknowledge matching fund from the Polish Ministry of Science and Higher Education No. 341832/PnH/2016.

REFERENCES

Akinlabi, E. O., Waclawczyk, M. & Malinowski, S. P. 2018 Fractal reconstruction of sub-grid scales for large eddy simulation of atmospheric turbulence. *Journal of Physics: Conference Series* .

- Akinlabi, E. O., Waclawczyk, Marta, Malinowski, Szymon P. & Mellado, Juan Pedro 2019 Fractal reconstruction of sub-grid scales for large eddy simulation. *Flow, Turbulence and Combustion* (Under revision).
- Barnley, M.F 1986 Constructive approximation 2 (303-329).
- Barnley, M.F 1993 Fractal everywhere. *Academy Press, Boston, MA* .
- Basu, S., Fofoula-Georgiou, E. & Porte-Agel, F. 2004 Synthetic turbulence, fractal interpolation and large eddy simulation. *Physical Review* **E70** (026310).
- Devroye, L. 1986 Non-uniform random variate generation. *Springer-Verlag New York Inc.* .
- Ishihara, T., T., Gotoh & Y., Kaneda 2009 Study of high-reynolds number isotropic turbulence by direct numerical simulation. *Annu. Rev. Fluid Mech.* **41** (165-180).
- Kamps, O., R., Friedrich & R., Grauer 2009 Exact relation between eulerian and lagrangian velocity increment statistics. *Phys. Fluids* **E79** (066301).
- Lui, L., F., Hu, X., Cheng & L., Song 2010 Probability density functions of velocity increments in the atmospheric boundary layer. *Boundary-Layer Meteorol.* **134** (243 - 255).
- Marchioli, C. 2017 Large eddy simulation of turbulent dispersed flows: a review of modelling approaches. *Acta Mech.* .
- Mazel, D. S. & Hayes, M. H. 1992 Using iterated function systems to model discrete sequences. *IEEE Transactions on signal processing* **40** (7).
- Mellado, J. P., van Heerwaarden C.C. & J.R., Garcia 2016 Near-surface effects of free atmosphere stratification in free convection. *Bound-layer Meteor.* (159), 69–95.
- Minier, J-P & Pozorski, J. 2017 Particles in wall-bounded turbulent flows: Deposition, re-suspension and agglomeration. *Springer* (571), 0254–1971.
- Orey, S. 1970 Gaussian sample functions and the hausdorff dimension of level crossings. *Z. Wahrscheinlichkeitstheorie Verw. Geb.* (15), 249 – 256.
- Praskovsky, A.A., J.F., Foss, S.J., Kleis & M.Y., Karyakin 1993 Fractal properties of isovelovity surfaces in high reynolds number laboratory shear flows. *Phys. Fluids* **A5** (2038-2042).
- Salvetti, M. V., Marchioli, C. & Soldati, A. 2006 Lagrangian tracking of particles in large eddy simulation with fractal interpolation. *Conference on Turbulence and Interactions TI2006* .
- Scotti, A., C., Meneveau & S.G., Saddoughi 1995 Fractal dimension of velocity signals in high reynolds number hydrodynamic turbulence. *Phys. Rev.* **E51** (5594 - 5608).
- Scotti, A. & Meneveau, C. 1999 A fractal model for large eddy simulation of turbulent flow. *Physica D* **127** (198232).
- Weinstein, C.J., IEEE Acoustics, Speech & Society, Signal Processing 1979 Digital signal processing committee programs for digital signal processing. *IEEE Press, New York* .